HHS Public Access

Author manuscript

Mol Cancer Ther. Author manuscript; available in PMC 2024 January 29.

Published in final edited form as:

Mol Cancer Ther. 2020 April ; 19(4): 1059–1069. doi:10.1158/1535-7163.MCT-19-0378.

Anti-Tumor Activity of the IGF-1/IGF-2-Neutralizing Antibody Xentuzumab (BI 836845) in Combination with Enzalutamide in Prostate Cancer Models

Ulrike Weyer-Czernilofsky[1], **Marco H. Hofmann**[1], **Katrin Friedbichler**[1], **Rosa Baumgartinger**[1], **Paul J. Adam**[1], **Flavio Solca**[1], **Norbert Kraut**[1], **Holly M. Nguyen**[2], **Eva Corey**[2], **Gang Liu**[3], **Cynthia C. Sprenger**[3], **Stephen R. Plymate**[3], **Thomas Bogenrieder**[1,4]

[1]Boehringer Ingelheim RCV GmbH & Co. KG, Vienna, Austria.

[2]Department of Urology, University of Washington, Seattle, Washington.

[3]Department of Medicine and GRECC VAPSHCS, University of Washington, Seattle, Washington.

[4]Department of Urology, University Hospital Grosshadern, Ludwig-Maximilians-University, Munich, Germany.

Abstract

Androgen deprivation therapy and second-generation androgen receptor signaling inhibitors such as enzalutamide (ENZA) are standard treatments for advanced/metastatic prostate cancer. Unfortunately, most men develop resistance and relapse; signaling via insulin-like growth factor (IGF) has been implicated in castration-resistant prostate cancer. We evaluated the anti-tumor

Corresponding Author: Ulrike Weyer-Czernilofsky, Boehringer Ingelheim RCV, Dr. Boehringer Gasse 5-11, 1121 Vienna, Austria. Phone: +43-664-88617566; Fax: +43-1-80105-32102; ulrike.weyer-czernilofsky@boehringer-ingelheim.com.
Current affiliations:
(Gang Liu) Mustang Bio, Inc. Worcester, Massachusetts
(Thomas Bogenrieder) Evaxion Biotech, Copenhagen, Denmark

Authors' Contributions

U. Weyer-Czernilofsky had full access to all the data in the study and takes responsibility for the integrity of the data and the accuracy of the data analysis.

Conception and design: U. Weyer-Czernilofsky, K. Friedbichler, P.J. Adam, F. Solca, N. Kraut, E. Corey, T. Bogenrieder, M.H. Hofmann

Acquisition of data (provided animals, acquired and managed patients, provided facilities, etc.): K. Friedbichler, R. Baumgartinger, P.J. Adam, H.M. Nguyen, E. Corey, G. Liu, C.C. Sprenger, S.R. Plymate

Analysis and interpretation of data (e.g., statistical analysis, biostatistics, computational analysis): U. Weyer-Czernilofsky, K. Friedbichler, R. Baumgartinger, P.J. Adam, F. Solca, E. Corey, G. Liu, C.C. Sprenger, S.R. Plymate, T. Bogenrieder, M.H. Hofmann

Writing, review, and/or revision of the manuscript: U. Weyer-Czernilofsky, K. Friedbichler, R. Baumgartinger, P.J. Adam, F. Solca, G. Liu, N. Kraut, H.M. Nguyen, E. Corey, C.C. Sprenger, S.R. Plymate, T. Bogenrieder, M.H. Hofmann

Administrative, technical, or material support (i.e., reporting or organizing data, constructing databases): U. Weyer-Czernilofsky, R. Baumgartinger

Study supervision: U. Weyer-Czernilofsky, N. Kraut, E. Corey, T. Bogenrieder, M.H. Hofmann

Disclosure of Potential Conflicts of Interest

U. Weyer-Czernilofsky, M.H. Hofmann, P.J. Adam, F. Solca, N. Kraut, and R. Baumgartinger are employees of Boehringer Ingelheim. T. Bogenrieder and K. Friedbichler are former employees of Boehringer Ingelheim. E. Corey, G. Liu, C.C. Sprenger, S.R. Plymate received research support from Boehringer Ingelheim. T. Bogenrieder holds ownership interest (including patents) in Roche, Seattle Genetics, Celgene, Gilead, and Immunogen. H.M. Nguyen declares no conflict of interest.

Availability of Materials and Data

All materials, data, and protocols described in the manuscript will be made available upon reasonable request, if the request is made within 6 years of publication. All data sets that were analyzed in the manuscript will be made available upon request to the Editors and peer-reviewers, and to the community at the time of publication.

Supplementary data for this article are available at Molecular Cancer Research Online (http://mcr.aacrjournals.org/).

activity of xentuzumab (XENT; IGF-ligand-neutralizing antibody), alone and in combination with ENZA, in prostate cancer cell lines (VCaP, DuCaP, MDA PCa 2b, LNCaP, PC-3) using established *in vitro* assays, and *in vivo*, using LuCaP 96CR, a prostate cancer patient-derived xenograft (PDX) model.

XENT+ENZA reduced the viability of phosphatase and tensin homolog (PTEN)-expressing VCaP, DuCaP, and MDA PCa 2b cells more than either single agent, and increased anti-proliferative activity and apoptosis induction in VCaP. XENT or XENT+ENZA inhibited IGF type 1 receptor (IGF-1R) and AKT serine/threonine kinase (AKT) phosphorylation in VCaP, DuCaP, and MDA PCa 2b cells; XENT had no effect on AKT phosphorylation and proliferation in *PTEN*-null LNCaP or PC-3 cells. Knockdown of PTEN led to loss of anti-proliferative activity of XENT and reduced activity of XENT+ENZA in VCaP cells. XENT+ENZA inhibited the growth of castration-resistant LuCaP 96CR PDX with acquired resistance to ENZA, and improved survival *in vivo*.

The data suggest that XENT+ENZA combination therapy may overcome castration resistance and could be effective in patients who are resistant to ENZA alone. PTEN status as a biomarker of responsiveness to combination therapy needs further investigation.

Keywords

BI 836845; castration-resistant prostate cancer; enzalutamide; IGF-ligand-neutralizing antibody; xentuzumab

Introduction

Worldwide, prostate cancer is the second most commonly diagnosed cancer and the fifth most common cause of cancer-related death among men, with 1,276,106 new cases and 358,989 deaths estimated in 2018 (1). The growth and survival of prostate cancer cells is androgen dependent, and androgen deprivation therapy (ADT) is standard treatment for advanced and metastatic prostate cancer (2). Unfortunately, most men relapse within 2 to 3 years despite achieving castrate serum androgen levels, and progress to a castration resistant state that precedes lethality (3, 4). The androgen receptor (AR) is an important mediator of castration resistance (3), as is the AR splice variant, AR variant 7 (AR-V7) (5), with AR signaling and transcriptional activity generally persisting in castration-resistant prostate cancer (CRPC), despite castrate levels of testosterone (2).

The second-generation androgen signaling inhibitor enzalutamide (ENZA; Xtandi®; MDV-3100) is a potent androgen antagonist. ENZA inhibits ligand binding to the AR, subsequent AR nuclear translocation, recruitment of AR co-activators and AR binding to DNA, and prevents transcription of essential genes that promote tumor growth (6) (https://www.medicines.org.uk/emc/product/10318/smpc). While ENZA has shown efficacy in CRPC, most patients develop resistance and some exhibit *de novo* resistance (7).

Signaling through the insulin-like growth factor (IGF) axis can contribute to castration-resistant disease via upregulation of IGF binding proteins and/or recovery of IGF type 1 receptor (IGF-1R) expression after castration (8). IGF-mediated phosphorylation or

dephosphorylation of specific AR sites may increase AR nuclear localization or decrease nuclear export, thereby enhancing AR signaling (9). Moreover, IGF induces transactivation of AR in the presence and absence of androgen (8, 9). Thus, there is a mechanistic rationale for combining IGF-targeted and anti-androgen therapy to attenuate tumor progression and improve survival in CRPC patients.

Xentuzumab (XENT; BI 836845; see ref (10) and Supplementary Methods for full sequence and structure) is a humanized monoclonal antibody (mAb) that binds IGF-1 and IGF-2, and neutralizes proliferative/anti-apoptotic signaling via IGF-1R and insulin receptor isoform A (INSR-A), without interfering with the metabolic effects of the INSR-B isoform or insulin (11). XENT has demonstrated potent anti-proliferative activity in preclinical studies (11), as well as manageable tolerability and encouraging single-agent activity in phase I trials in patients with advanced solid tumors (12, 13).

The objectives of this study were to investigate the *in vitro* and *in vivo* anti-tumor activity of XENT in combination with ENZA in models of human prostate cancer.

Materials and Methods

Test compounds

XENT was produced at Boehringer Ingelheim Pharma GmbH & Co KG, Biberach, Germany. ENZA was synthesized at TCG Lifesciences Ltd, India. For *in vivo* studies, ENZA was formulated with 0.5% Natrosol™, and the suspension for dosing was stored in the dark at room temperature for up to 5 days; XENT was administered as provided.

Cell lines

Human prostate cancer cell lines, LNCaP (clone FGC), MDA PCa 2b, PC-3, and VCaP were obtained from the American Type Culture Collection (ATCC). DuCaP cells were kindly provided by Prof. Dr Helmut Klocker, University Hospital Innsbruck, Austria. Research Resource Identifiers are provided in the Supplementary Information. All cell lines were further authenticated by short tandem repeat (STR) analysis at Boehringer Ingelheim prior to use, and were regularly tested for mycoplasma (MycoAlert Mycoplasma Detection Kit, Lonza) (see Supplementary Table S1). New batches of cell lines were regularly thawed, i.e. after approximately 20 passages/2–3 months in culture. See Supplementary Methods for details of cell culture conditions.

All investigated cell lines express IGF-1R; AR expression was detectable in all except PC-3 cells. VCaP and DuCaP are phosphatase and tensin homolog (*PTEN*) wild-type, MDA PCa 2b cells harbor a heterozygous *PTEN* mutation, and LNCaP and PC-3 are *PTEN*-null. PTEN protein is expressed by VCaP, DuCaP, and MDA PCa 2b, but not by LNCaP or PC-3 (Supplementary Fig. S1A).

Cell viability and proliferation assays

Cell viability was measured using the CellTiter-Glo® Luminescent Assay (Promega). Briefly, cells were seeded onto non-transparent 96-well plates, and treated with indicated concentrations of XENT and ENZA in medium supplemented with fetal bovine serum (FBS)

the following day. All samples were tested with three technical replicates. Plates were incubated for 5 days (DuCaP, MDA PCa 2b), 7 days (LNCaP), or 10 days (VCaP, PC-3). For 10-day treatment, XENT and ENZA administration was repeated after 5 days. At the time of first drug administration, a “time zero” (T0) untreated cell plate was measured. Luminescence intensity was read using a microplate reader. For data analysis, the mean value from triplicate wells was taken and fitted by iterative calculations using a sigmoidal curve analysis program (Graph Pad Prism) with variable Hill slope.

In addition, the effect of drug treatment on the proliferation on VCaP cells was assessed using a thymidine incorporation assay. Cells were treated with indicated concentrations of XENT and ENZA in medium containing FBS for 96 hours. ^{3}H-thymidine (0.4 μCi/well) was added for the last 24 hours. Thymidine incorporation was determined using a liquid scintillation counter (Wallac 1450 MicroBeta TriLux, PerkinElmer).

Western blot, Simple Western™ and quantitative polymerase chain reaction (qPCR) analyses

For analysis of IGF signaling and apoptosis markers, prostate cancer cells were seeded in medium supplemented with 10% FBS, incubated overnight, and treated with the indicated concentrations of XENT, ENZA, or both.

For analysis of AR signaling markers, VCaP cells were seeded in medium with 10% charcoal-stripped serum, incubated overnight, and treated with XENT, ENZA, or both for 22 hours (qPCR) or 46 hours (Western blots). Synthetic androgen R1881 (0.1 nM) was added 2 hours after treatment start.

Cells were lysed at various time points post-treatment and analyzed by Western blot, Simple Western™, or qPCR (see Supplementary Methods and Supplementary Table S2 for further details).

Cell-cycle analysis

VCaP cells were treated with XENT (1 μM), ENZA (10 μM), or both, and incubated at 37°C for 24, 48, and 72 hours. Cells were fixed in ice-cold 70% ethanol for ≥2 hours at 4°C, washed in phosphate-buffered saline and incubated in hypotonic buffer solution (0.1% sodium citrate, 0.1% (v/v) triton-X100, 100 μg/mL DNase-free RNase A) and propidium iodide (10 μg/mL) for 30 min at room temperature in the dark. Cells were analyzed by flow cytometry on the fluorescence-activated cell sorting (FACS) Canto II flow cytometer (Becton Dickinson). Data were evaluated with FACS Diva software (Becton Dickinson).

Caspase 3/7 activity

VCaP cells were treated with XENT (0.1 μM or 1 μM), ENZA (1 μM or 10 μM), or XENT+ENZA and incubated at 37°C for 96 hours. Caspase 3/7 activity was assayed in at least triplicate using the IncuCyte® Caspase 3/7 Reagent (Essen Bioscience), according to the manufacturer’s instructions. Kinetic measures of the number of caspase 3/7 positive cells was recorded over time and plotted as signals per mm^{2}.

In vivo study in LuCaP 96CR patient-derived xenograft (PDX) model

Fox Chase CB17 severe combined immunodeficiency (SCID; CB17/lcr-Prkdc scid/lcrlcoCrl) male mice (4 to 8 weeks old; Charles River) were castrated and implanted with LuCaP 96CR (castration-resistant) tumor fragments 2 weeks later (see Supplementary Methods). Once tumor volumes exceeded 101 mm^3, animals were randomized to receive Natrosol™ vehicle control (orally [p.o.]; $n = 15$), ENZA (30 mg/kg p.o.; 5 days on, 2 days off, for 10 cycles; $n = 15$), or ENZA (dosing regimen as previously noted) plus XENT (200 mg/kg intraperitoneally [i.p.], once weekly for 10 cycles; $n = 14$). Serum prostate-specific antigen (PSA [KLK3; kallikrein related peptidase 3]) was measured using the Architect Total PSA Assay (Abbott Laboratories). Animals were sacrificed either after 10 weeks of treatment (6 hours after the last dose), when tumors had exceeded 1,000 mm^3, when weight loss exceeded 20%, or when otherwise compromised [as defined by the University of Washington Institutional Animal Care and Use Committee protocol (Seattle, WA)]. Tumors were then harvested and processed for analysis (see Supplementary Methods). All animal studies were approved by the internal ethics committee and the local governmental committee.

Additional materials and methods

Details of analysis of PTEN status of LuCaP 96CR, RNA interference, statistical analysis of *in vitro* assays, RNA isolation and qPCR analysis of tumor samples, RNA-Seq, gene set enrichment analysis (GSEA), and immunohistochemistry (IHC) are described in the Supplementary Methods. RNA-seq and microarray data for the LuCaP 96CR PDX model are deposited in the GEO (GSE124704, GSM2462884, GSM2462771, GSM2462795).

Results

Anti-proliferative effect of IGF and AR signaling blockade in prostate cancer cell lines

The XENT+ENZA combination was tested in a set of prostate cancer cell lines. The viability of VCaP, DuCaP, and MDA PCa 2b cells was reduced by single-agent XENT or ENZA in a dose-dependent manner, after 5 or 10 days of incubation. Combination treatment further reduced cell viability versus the single agents (as shown in Fig. 1A-C, these reductions were statistically significant). In contrast, in LNCaP cells, XENT+ENZA provided no greater inhibition than ENZA alone, and single-agent XENT exhibited no anti-proliferative effects (Fig. 1D); both agents (alone and combined) were inactive in PC-3 cells (Fig. 1E). The greater anti-proliferative effect of combination treatment was confirmed by measuring thymidine incorporation in VCaP cells (Fig. 1F). The notion that addition of XENT enhanced the activity of ENZA in three *PTEN*-wild-type cell lines but not in *PTEN*-null LNCaP cells prompted us to investigate the effect of PTEN knockdown in VCaP cells. RNA interference-mediated silencing resulted in complete loss of anti-proliferative activity of XENT, and reduced the activity of XENT+ENZA to the level observed with ENZA alone, demonstrating that functional PTEN is required for combinatorial activity in the VCaP cell line (Fig. 1G; Supplementary Fig. S2A and B).

Inhibitory effects on IGF-1R and AR signaling

XENT inhibited IGF-1R phosphorylation in all five cell lines (Fig. 2; Supplementary Fig. S1B-E). Both XENT and combination treatment suppressed AKT serine/threonine kinase (AKT) phosphorylation in VCaP (Fig. 2), DuCaP, and MDA PCa 2b (Supplementary Fig. S1B and C), but not in LNCaP or PC-3 *PTEN*-null (Supplementary Fig. S1D and E). ENZA had little effect on IGF-1R and AKT phosphorylation in any of the cell lines.

VCaP cells were selected to further investigate the effects of XENT+ENZA; these cells recapitulate the relative expression levels of full-length AR (AR-FL) and AR-Vs observed in clinical CRPC specimens, that is, detectable but lower levels of AR-Vs than AR-FL (14).

XENT alone did not affect expression of AR-regulated genes in VCaP cells. In line with its mechanism of action, ENZA (±XENT) markedly reduced transcript and protein levels of AR-regulated target genes, namely PSA, FK506 binding protein 5 (FKBP5 [FKBP prolyl isomerase 5]), transmembrane serine protease 2 (TMPRSS2), and ETS related gene (ERG [ETS transcription factor ERG]) (Supplementary Fig. S3A). Treatment with XENT+ENZA led to the most pronounced reduction in expression of the cell-cycle genes, ubiquitin-conjugating enzyme E2 C (UBE2C), cyclin-dependent kinase 1 (CDK1), and cell-division cycle protein 20 (CDC20) (Supplementary Fig. S3B).

Effect of IGF and AR signaling blockade on cell-cycle profile and induction of apoptosis

XENT increased the sub-G1 cell population (indicative of apoptotic cells) over time compared with untreated VCaP controls (25% vs. 10% after 3 days); XENT+ENZA further enhanced this population to 44% after 3 days (Fig. 3). ENZA alone had only minor effects on the cell-cycle profile of VCaP cells. XENT produced a minor (with 0.1 μM) or moderate (with 1 μM) increase in cleaved caspase 3/7, while ENZA (1 and 10 μM) did not affect caspase 3/7 activity over time versus control (Fig. 4A and C; Supplementary Fig. S4A). In combination, XENT+ENZA significantly enhanced caspase activity compared with either single agent. Cleavage of poly(adenosine diphosphate-ribose) polymerase (PARP) was only apparent after combination treatment (Fig. 4B and C).

To further elucidate the mechanism of increased apoptosis, treatment effects on regulators of apoptosis were investigated. XENT and XENT+ENZA inhibited the phosphorylation of well-established direct substrates of AKT, namely the Forkhead box O (FoxO) transcription factors, FoxO3a and FoxO1 (important regulators of expression of genes involved in apoptosis; Fig. 4C), and the BH3-only pro-apoptotic protein, Bcl2-associated agonist of cell death (Bad; Fig. 4D). Minor treatment effects were observed on total protein expression levels of FoxOs, and other pro- and anti-apoptotic factors, Bcl-2-like protein 4 (Bax [BCL2 associated X, apoptosis regulator]), Bcl-2 antagonist/killer (Bak), Bcl-2-like protein 11 (Bim [BCL2L11; BCL2 like 11]), and B-cell lymphoma-extra large (Bcl-XL) (Supplementary Fig. S4B).

In vivo activity of XENT and ENZA

The anti-tumor activity of XENT+ENZA was evaluated using the LuCaP 96CR PDX model, which mimics CRPC with acquired resistance to the standard-of-care agent, ENZA.

Whereas, as expected, ENZA monotherapy did not inhibit tumor growth, addition of XENT re-sensitized tumors to ENZA and resulted in significant reductions in tumor volume (Fig. 5A and B). All mice treated with the combination were alive at the end of the study (> 10 weeks), representing a significant survival improvement versus ENZA alone (Fig. 5C). Treatment with ENZA or the combination for 2 weeks resulted in a trend toward decreased serum PSA versus control (Fig. 5D). At sacrifice, the reduction in PSA with combination treatment was statistically significant versus control (~65%, $P = 0.033$), but not versus ENZA alone ($P = 0.079$).

Analysis of tumor samples

At the end of the LuCaP 96CR efficacy study (at sacrifice), tumors were harvested (6 hours after the last dose) and processed for analysis. ENZA significantly increased AR-FL mRNA and protein versus control, and only moderate further increases occurred with combination therapy (Supplementary Fig. S5A and C). In contrast, AR-V7 mRNA was significantly increased by XENT+ENZA compared with ENZA alone (Supplementary Fig. S5A), and this finding was confirmed at the protein level using IHC (Supplementary Fig. S5B). Of note, compared with control, combination treatment significantly reduced transcripts of UBE2C (a mitotic [M]-phase cell-cycle gene regulated by AR-V7), while ENZA alone had no significant effect (Fig. 6A).

RNA-Seq and GSEA analyses of ENZA- and combination-treated LuCaP 96CR tumors (Fig. 6B-E; Supplementary Table S3) showed that ENZA-activated or -suppressed targets were further altered when XENT was added; eight genes were upregulated and 29 genes downregulated (Fig. 6B). The GSEA results of all C2-canonical pathways with false discovery rate (FDR) < 0.05 (133 negatively; 81 positively enriched) are detailed in Supplementary Table S3; all Hallmark pathways with FDR < 0.05 (27 negatively; six positively enriched) are shown in Fig. 6C. Compared with ENZA alone, the hypoxia-inducible factor-1-alpha (HIF-1-α [HIF1A; hypoxia inducible factor 1 subunit alpha]) transcription factor network (Fig. 6D) and the closely-related hypoxia gene set (Fig. 6C) were significantly downregulated by the combination, as was the androgen response gene set (Fig. 6E). Other negatively enriched pathways included extracellular matrix, adhesion, epithelial–mesenchymal transition networks, and signaling pathways such as Wnt and Notch (Fig. 6C; Supplementary Table S3). Positively enriched pathways included E2F transcription factors, MYC targets Version 1 and 2, and the G2M checkpoint (Fig. 6C; Supplementary Table S3).

Discussion

The lack of a durable response to androgen- or AR-targeted therapy is a major challenge in CRPC management (7). Transactivation of AR by growth factors and cytokines is one of many mechanisms that drive progression to castration resistance (15). IGF-1R-mediated activation of the phosphoinositide 3-kinase/AKT pathway is one of the proposed mechanisms for AR transactivation under castrated conditions (15), the presence of which supports co-targeting of the AR and IGF-1R pathways in patients with CRPC.

Our data *in vitro* show that XENT+ENZA reduces proliferation more effectively than either treatment alone in PTEN-positive prostate cancer cells. In VCaP cells, requirement of functional PTEN for combinatorial anti-proliferative activity was demonstrated by PTEN knockdown. LuCaP 96CR harbors loss of one copy of the *PTEN* gene, and a deletion of exon 3 on the other allele, but it is possible that PTEN in LuCaP 96CR may still retain functional phosphatase activity, since exon 3 loss does not disrupt the active site (Supplementary Fig. S6). Interestingly, a clinical trial of the IGF-1R targeting mAb ganitumab failed to establish a correlation between clinical benefit and PTEN status (but most tumor samples were PTEN-positive) (16). Likewise, suppression of IGF-1R expression with an antisense oligonucleotide reduced proliferation and increased apoptosis of *PTEN*-null PC-3 and LNCaP cells (17). The mechanisms of increased apoptosis after knockdown of IGF-1R in *PTEN*-null cell lines are not yet understood, particularly as IGF-1/2 neutralization does not result in similar effects. These differences may be explained by the distinct capability of IGF-1R-targeted agents and IGF ligand-blocking antibodies to affect proliferative and survival signaling downstream of homo- and hetero-dimers of the IGF/INSR family (18). Our finding that XENT failed to inhibit AKT phosphorylation in LNCaP or PC-3 *PTEN*-null cells suggests that the lack of anti-proliferative activity may reflect the failure of XENT to inhibit downstream IGF ligand-independent signaling in these cells. Taken together, the impact of PTEN status on response to XENT+ENZA in CRPC requires further investigation.

XENT+ENZA treatment was shown to exert its combinatorial activity through enhanced tumor cell apoptosis. These findings are in line with the key role of IGF signaling in conferring a survival response that acts as a resistance mechanism, limiting the effectiveness of cytotoxic or targeted anti-cancer agents. Mechanistically, XENT induced the intrinsic apoptotic pathway by affecting the phosphorylation status of AKT and downstream pro-apoptotic regulators, BH3-only protein Bad and transcription factors FoxO3a and FoxO1, on residues reported to be AKT substrates. Specifically, inhibition of Bad phosphorylation on serine residues S136 and S112 by XENT and XENT+ENZA is in line with reports that suppression of Bad activity by IGF-1R/AKT signaling involves phosphorylation on these residues (19, 20), and inhibition of FoxO protein phosphorylation occurred at threonine and serine residues regulated by AKT (FoxO3a: T32 and S253; FoxO1: T24) (21, 22). Total protein levels of apoptotic regulators were largely unaffected in our studies, which is concordant with published evidence suggesting that other pathways, such as p53 and nuclear factor kappa-light-chain-enhancer of activated B cells (NF-κB), play important roles in regulating gene expression of pro- and anti-apoptotic factors (23-25).

The observation that progression of ENZA-resistant LuCaP 96CR PDX was inhibited by the combination treatment versus controls, together with the survival benefit with the combination versus single-agent ENZA, supports available evidence that the augmented anti-tumor effects of IGF- and AR-targeted combinations translate into enhanced *in vivo* efficacy (8, 26). For example, the anti-IGF-1R antibody A12 enhanced tumor regression *in vivo* and prolonged survival after castration (8). In our study, the *in vivo* anti-tumor efficacy of combination treatment was not accompanied by significant suppression of serum PSA levels versus ENZA alone, suggesting that serum PSA level may not be an appropriate indicator of XENT activity in CRPC clinical trials.

In LuCaP 96CR tumor samples taken at the end of the efficacy study, increased AR-V7 expression levels were observed in the XENT+ENZA group compared with the ENZA-only group. Interestingly, clinical data have shown an upregulation of AR-V7 as a treatment response to ENZA or abiraterone acetate in CRPC patients (27). While the mechanism behind the increase in AR-V7 upon XENT+ENZA treatment in our study remains unclear, we speculate that it likewise reflects an adaptive response upon therapy. Regardless of upregulated AR-V7 at study end, a downregulation of AR response pathways (GSEA) and of UBE2C expression (qPCR) in the presence of XENT+ENZA compared with ENZA alone was demonstrated. Suppression of the M phase checkpoint UBE2C, on one hand, reflects anti-proliferative activity elicited by XENT+ENZA (consistent with the reduction in tumor growth), but, in addition, may indicate reduced transcriptional activity of AR-V7. UBE2C is reported to be a representative target gene of AR-V7 under androgen-depleted conditions (28, 29), with its expression being specifically regulated by AR-V7 and not by AR-FL, both in prostate cancer cells and in tissues from CRPC patients (30). In light of the significant tumor growth delay and clear survival benefit observed with combination treatment at the end of the experiment, the upregulation of E2F and MYC targets revealed by GSEA seems counterintuitive. Our interpretation is that, after long-term treatment for up to 10 weeks, tumor samples are not representative of acute pharmacodynamic effects of the drugs but, rather, mirror a steady state, reflecting compensatory mechanisms. E2F and MYC are not bona fide oncogenic drivers, but their upregulation may support tumor cell survival at this late time point. Investigation of counter-regulatory mechanisms in response to XENT+ENZA treatment has important translational relevance and will be a focus of future studies.

Interestingly, the HIF-1α/hypoxia pathway was one of the pathways downregulated most by ENZA+XENT. IGF-1R signaling regulates HIF-1α and protects tumor cells from the negative effects of hypoxia (31). Consequently, downregulation of the HIF-1α pathway may contribute to anti-tumor efficacy of XENT+ENZA combination therapy.

Our results support two potential strategies for more effective inhibition of the IGF/IGF-1R signaling axis in CRPC. The first strategy is that of concurrent administration of IGF-1/−2 ligand-neutralizing antibodies such as XENT with androgen signaling inhibitors, the objective being to prevent the IGF-stimulated resistance pathway from driving prostate cancer progression, by inhibiting AR-V7 transcriptional activity (among other mechanisms). Indeed, it was recently shown that IGF-1R is a primary target of both the AR-FL and AR-V7 cistrome (32). The marked increase in AR-V7 following ENZA treatment is an important and frequent mechanism of resistance to androgen-directed therapies; AR-V7 is expressed in less than 1% of primary prostate cancer (castration-sensitive) but at least 75% of castration-resistant tumors (27). Our results showed reduced expression of AR-V7-regulated genes following combination treatment, consistent with the previous findings that inhibition of IGF-1R by the tyrosine kinase inhibitors NVP-AEW541 and AG1024 led to downregulation of AR-V7 transcriptional activity in prostate cancer cells (33). The second potential strategy employs a more precision-based approach, using candidate biomarkers such as PTEN and AR-V7 to aid patient enrichment.

In conclusion, reciprocal reactivation of IGF and AR signaling in response to AR/IGF-inhibitor-mediated feedback provides a rationale for simultaneous targeting of both pathways in AR- and/or IGF-dependent tumors. In our studies, combined treatment with anti-AR and anti-IGF-1/−2 therapies produced concurrent suppression of AR signaling and compensatory IGF/IGF-1R activity. The combination of these effects led to enhanced anti-proliferative/pro-apoptotic effects *in vitro*, and significant *in vivo* efficacy in a PDX model of castration- and ENZA-resistant prostate cancer. Further *in vivo* studies will investigate the emergence of counter-regulatory mechanisms arising during treatment, and may identify suitable enrichment biomarkers (e.g., PTEN status, IGF-1/2 levels, TMPRSS2-ERG [T2E] fusion gene expression, or AR-V7 gene expression) for selection of patients who would be most likely to benefit from this combination therapy.

Supplementary Material

Refer to Web version on PubMed Central for supplementary material.

Acknowledgments

We thank Dr. Daniel Gerlach, Boehringer Ingelheim RCV GmbH & Co. KG, Vienna, Austria, for support in analysis of the *PTEN* status of LuCaP 96CR, Daniela Fürweger and Ulrike Nagl, Boehringer Ingelheim RCV GmbH & Co. KG, Vienna, Austria, for performing several of the experiments, and Prof. Dr Helmut Klocker, University Hospital Innsbruck, Austria, for provision of DuCaP cells. Medical writing assistance, supported financially by Boehringer Ingelheim, was provided by Fiona Scott, of GeoMed, an Ashfield company, part of UDG Healthcare plc, during the preparation of this article.

The studies were supported by Boehringer Ingelheim RCV GmbH & Co. KG and the Veterans Affairs Research Program (SRP). Establishment and maintenance of the LuCaP patient-derived xenografts by E. Corey and H. Nguyen was supported by the Pacific Northwest Prostate Cancer SPORE (Grant Reference Number: P50 CA097186), the ProGMap Project (Grant Reference Number: P01 CA163227), the Prostate Cancer Foundation, and the Richard M. Lucas Foundation.

Abbreviations list for main paper:

ADT	androgen deprivation therapy
AKT	AKT serine/threonine kinase
AR	androgen receptor
AR-FL	full-length AR
AR-V7	AR variant 7
ATCC	American Type Culture Collection
Bad	Bcl2-associated agonist of cell death
Bak	Bcl-2 antagonist/killer
Bax	Bcl-2-like protein 4 (BCL2 associated X, apoptosis regulator)
Bcl-XL	B-cell lymphoma-extra large
Bim	Bcl-2-like protein 11 (BCL2L11; BCL2 like 11)

CDC20	cell division cycle protein 20
CDK1	cyclin-dependent kinase 1
CRPC	castration-resistant prostate cancer
ENZA	enzalutamide
ERG	ETS related gene (ETS transcription factor ERG)
FACS	fluorescence-activated cell sorting
FKBP5	FK506 binding protein 5 (FKBP prolyl isomerase 5)
FoxO1	Forkhead box O1
FoxO3a	Forkhead box O3a
FBS	fetal bovine serum
FDR	false discovery rate
GSEA	gene set enrichment analysis
HIF-1-α	hypoxia-inducible factor-1-alpha (HIF1A; hypoxia inducible factor 1 subunit alpha)
IGF	insulin-like growth factor
IGF-1R	IGF type 1 receptor (IGF1R; insulin like growth factor 1 receptor)
IHC	immunohistochemistry
INSR	insulin receptor
i.p.	intraperitoneally
mAb	monoclonal antibody
M	mitotic
NES	normalized enrichment score
NF-κB	nuclear factor kappa-light-chain-enhancer of activated B cells
PARP	poly(adenosine diphosphate-ribose) polymerase
PDX	patient-derived xenograft
phospho	phosphorylated
p.o.	orally
PSA	prostate-specific antigen (KLK3; kallikrein related peptidase 3)
PTEN	phosphatase and tensin homolog

qPCR	quantitative polymerase chain reaction
SCID	severe combined immunodeficiency
siRNA	small interfering RNA
STR	short tandem repeat
T2E	TMPRSS2-ERG
TMPRSS2	transmembrane serine protease 2
UBE2C	ubiquitin-conjugating enzyme E2 C
XENT	xentuzumab

References

1. Bray F, Ferlay J, Soerjomataram I, Siegel RL, Torre LA, Jemal A. Global cancer statistics 2018: GLOBOCAN estimates of incidence and mortality worldwide for 36 cancers in 185 countries. CA Cancer J Clin 2018;68:394–424. [PubMed: 30207593]
2. Yuan X, Cai C, Chen S, Chen S, Yu Z, Balk SP. Androgen receptor functions in castration-resistant prostate cancer and mechanisms of resistance to new agents targeting the androgen axis. Oncogene 2014;33:2815–25. [PubMed: 23752196]
3. Chandrasekar T, Yang JC, Gao AC, Evans CP. Mechanisms of resistance in castration-resistant prostate cancer (CRPC). Transl Androl Urol 2015;4:365–80. [PubMed: 26814148]
4. Seruga B, Tannock IF. Chemotherapy-based treatment for castration-resistant prostate cancer. J Clin Oncol 2011;29:3686–94. [PubMed: 21844499]
5. Antonarakis ES, Lu C, Wang H, Luber B, Nakazawa M, Roeser JC, et al. AR-V7 and resistance to enzalutamide and abiraterone in prostate cancer. N Engl J Med 2014;371:1028–38. [PubMed: 25184630]
6. Beer TM, Tombal B. Enzalutamide in metastatic prostate cancer before chemotherapy. N Engl J Med 2014;371:1755–56.
7. Pal SK, Patel J, He M, Foulk B, Kraft K, Smirnov DA, et al. Identification of mechanisms of resistance to treatment with abiraterone acetate or enzalutamide in patients with castration-resistant prostate cancer (CRPC). Cancer 2017;124:1216–24. [PubMed: 29266182]
8. Plymate SR, Haugk K, Coleman I, Woodke L, Vessella R, Nelson P, et al. An antibody targeting the type I insulin-like growth factor receptor enhances the castration-induced response in androgen-dependent prostate cancer. Clin Cancer Res 2007;13:6429–39. [PubMed: 17975155]
9. Wu JD, Haugk K, Woodke L, Nelson P, Coleman I, Plymate SR. Interaction of IGF signaling and the androgen receptor in prostate cancer progression. J Cell Biochem 2006;99:392–401. [PubMed: 16639715]
10. World Health Organization. Recommended international nonproprietary names, list 76. WHO Drug Information 2016;30:359–544. Available from: http://apps.who.int/medicinedocs/documents/s23010en/s23010en.pdf.
11. Friedbichler K, Hofmann MH, Kroez M, Ostermann E, Lamche HR, Koessl C, et al. Pharmacodynamic and antineoplastic activity of BI 836845, a fully human IGF ligand-neutralizing antibody, and mechanistic rationale for combination with rapamycin. Mol Cancer Ther 2014;13:399–409. [PubMed: 24296829]
12. Doi T, Shitara K, Naito Y, Kuboki Y, Kojima T, Hosono A, et al. Phase I dose escalation trial of weekly intravenous xentuzumab (BI 836845) in Japanese patients with advanced solid tumors. Ann Oncol 2016;27(Suppl):abstract 2790.
13. Rihawi K, Ong M, Michalarea V, Bent L, Buschke S, Bogenrieder T, et al. Phase I dose escalation study of 3-weekly BI 836845, a fully human, affinity optimized, insulin-like growth factor (IGF)

ligand neutralizing antibody, in patients with advanced solid tumors. J Clin Oncol 2014;32(Suppl 5):abstract 2622.

14. Hu R, Dunn TA, Wei S, Isharwal S, Veltri RW, Humphreys E, et al. Ligand-independent androgen receptor variants derived from splicing of cryptic exons signify hormone-refractory prostate cancer. Cancer Res 2009;69:16–22. [PubMed: 19117982]
15. Wu J, Yu E. Insulin-like growth factor receptor-1 (IGF-IR) as a target for prostate cancer therapy. Cancer Metastasis Rev 2014;33:607–17. [PubMed: 24414227]
16. Rosen LS, Puzanov I, Friberg G, Chan E, Hwang YC, Deng H, et al. Safety and pharmacokinetics of ganitumab (AMG 479) combined with sorafenib, panitumumab, erlotinib, or gemcitabine in patients with advanced solid tumors. Clin Cancer Res 2012;18:3414–27. [PubMed: 22510349]
17. Furukawa J, Wraight CJ, Freier SM, Peralta E, Atley LM, Monia BP, et al. Antisense oligonucleotide targeting of insulin-like growth factor-1 receptor (IGF-1R) in prostate cancer. Prostate 2010;70:206–18. [PubMed: 19790231]
18. Simpson A, Petnga W, Macaulay VM, Weyer-Czernilofsky U, Bogenrieder T. Insulin-like growth factor (IGF) pathway targeting in cancer: role of the IGF axis and opportunities for future combination studies. Target Oncol 2017;12:571–97. [PubMed: 28815409]
19. Peruzzi F, Prisco M, Dews M, Salomoni P, Grassilli E, Romano G, et al. Multiple signaling pathways of the insulin-like growth factor 1 receptor in protection from apoptosis. Mol Cell Biol 1999;19:7203–15. [PubMed: 10490655]
20. Sastry KS, Smith AJ, Karpova Y, Datta SR, Kulik G. Diverse antiapoptotic signaling pathways activated by vasoactive intestinal polypeptide, epidermal growth factor, and phosphatidylinositol 3-kinase in prostate cancer cells converge on BAD. J Biol Chem 2006;281:20891–901. [PubMed: 16728406]
21. Brunet A, Bonni A, Zigmond MJ, Lin MZ, Juo P, Hu LS, et al. Akt promotes cell survival by phosphorylating and inhibiting a Forkhead transcription factor. Cell 1999;96:857–68. [PubMed: 10102273]
22. Dobson M, Ramakrishnan G, Ma S, Kaplun L, Balan V, Fridman R, et al. Bimodal regulation of FoxO3 by AKT and 14-3-3. Biochim Biophys Acta 2011;1813:1453–64. [PubMed: 21621563]
23. Miyashita T, Reed JC. Tumor suppressor p53 is a direct transcriptional activator of the human bax gene. Cell 1995;80:293–9. [PubMed: 7834749]
24. Graupner V, Alexander E, Overkamp T, Rothfuss O, De Laurenzi V, Gillissen BF, et al. Differential regulation of the proapoptotic multidomain protein Bak by p53 and p73 at the promoter level. Cell Death Differ 2011;18:1130–9. [PubMed: 21233848]
25. Chen C, Edelstein LC, Gelinas C. The Rel/NF-kappaB family directly activates expression of the apoptosis inhibitor Bcl-x(L). Mol Cell Biol 2000;20:2687–95. [PubMed: 10733571]
26. Mancarella C, Casanova-Salas I, Calatrava A, Ventura S, Garofalo C, Rubio-Briones J, et al. ERG deregulation induces IGF-1R expression in prostate cancer cells and affects sensitivity to anti-IGF-1R agents. Oncotarget 2015;6:16611–22. [PubMed: 25906745]
27. Sharp A, Coleman I, Yuan W, Sprenger C, Dolling D, Nava Rodrigues D, et al. Androgen receptor splice variant-7 expression emerges with castration resistance in prostate cancer. J Clin Invest 2018;129:192–208. [PubMed: 30334814]
28. Lee CH, Ku JY, Ha JM, Bae SS, Lee JZ, Kim CS, et al. Transcript levels of androgen receptor variant 7 and ubiquitin-conjugating enzyme 2C in hormone sensitive prostate cancer and castration-resistant prostate cancer. Prostate 2017;77:60–71. [PubMed: 27550197]
29. Wang Q, Li W, Zhang Y, Yuan X, Xu K, Yu J, et al. Androgen receptor regulates a distinct transcription program in androgen-independent prostate cancer. Cell 2009;138:245–56. [PubMed: 19632176]
30. Boudadi K, Suzman DL, Anagnostou V, Fu W, Luber B, Wang H, et al. Ipilimumab plus nivolumab and DNA-repair defects in AR-V7-expressing metastatic prostate cancer. Oncotarget 2018;9:28561–71. [PubMed: 29983880]
31. Mimeault M, Batra SK. Hypoxia-inducing factors as master regulators of stemness properties and altered metabolism of cancer- and metastasis-initiating cells. J Cell Mol Med 2013;17:30–54. [PubMed: 23301832]

32. Cato L, de Tribolet-Hardy J, Lee I, Rottenberg JT, Coleman I, Melchers D, et al. ARv7 represses tumor-suppressor genes in castration-resistant prostate cancer. Cancer Cell 2019;35:401–13.e6. [PubMed: 30773341]

33. Zengerling F, Azoitei A, Herweg A, Jentzmik F, Cronauer MV. Inhibition of IGF-1R diminishes transcriptional activity of the androgen receptor and its constitutively active, C-terminally truncated counterparts Q640X and AR-V7. World J Urol 2016;34:633–9. [PubMed: 26318637]

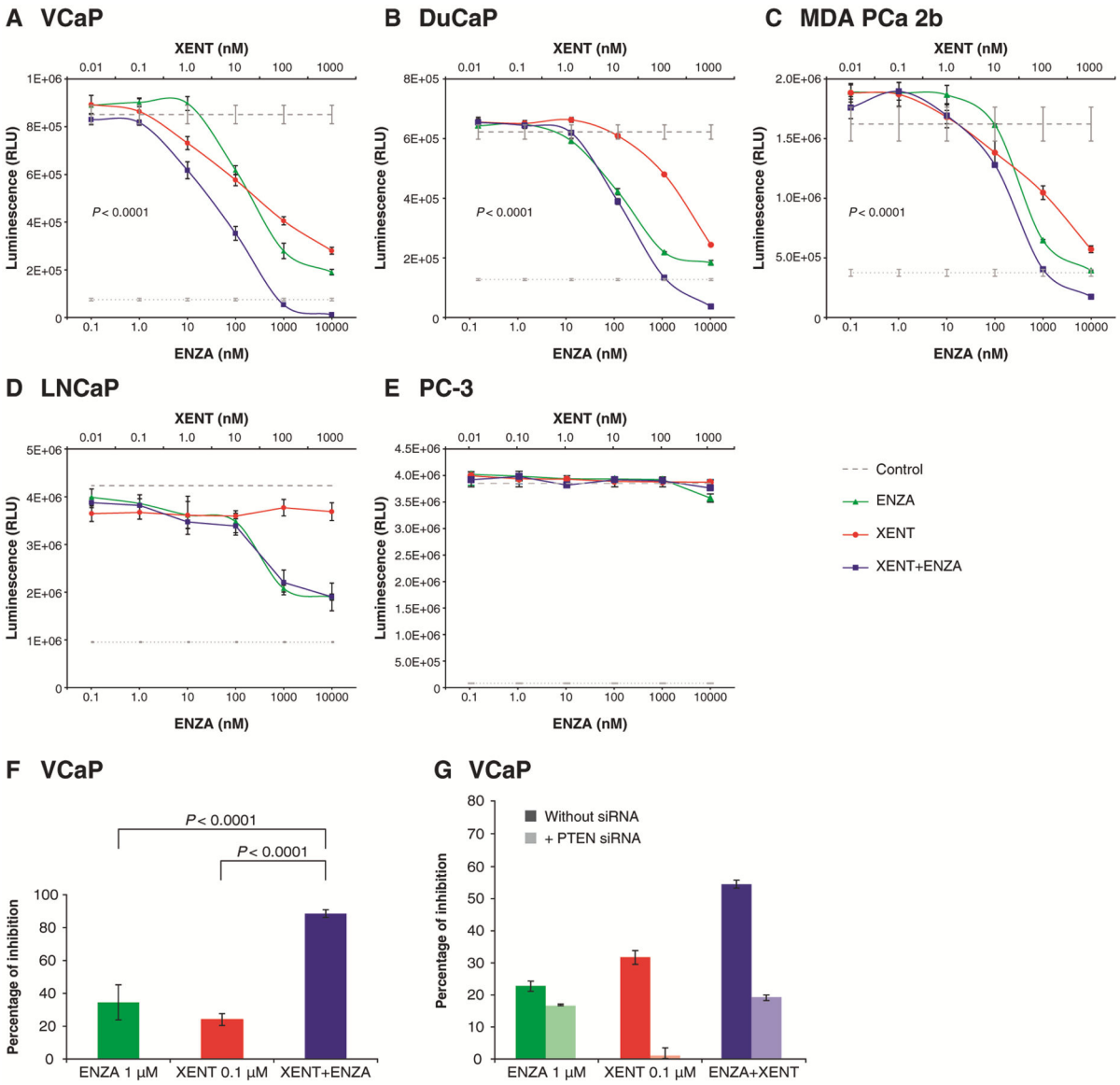

Figure 1.

Effects of XENT and ENZA, alone or in combination, on prostate cancer cells: A–E) Cells were cultivated in medium containing FBS, in the absence of androgen or growth factor supplementation, and cell viability was measured using the CellTiter-Glo® Luminescent Assay after treatment with indicated concentrations of XENT and ENZA for 5 days (DuCaP, MDA PCa 2b), 7 days (LNCaP), or 10 days (VCaP, PC-3). F) VCaP cell proliferation was determined by measuring thymidine incorporation in a 5 day assay in FBS-containing medium. G) VCaP cells were either left untransfected or were transfected with PTEN small interfering RNA (siRNA), and were treated with XENT, ENZA, or XENT+ENZA. Cell viability was measured after 3 days using the CellTiter- Glo® Assay. Results are represented as percentage of inhibition, relative to untreated control, with or without PTEN siRNA, respectively. Data are expressed as mean ± standard deviation for n = 3. *P* values were

calculated using pairwise t-tests (adjusted for multiplicity) following a one-way analysis of variance.

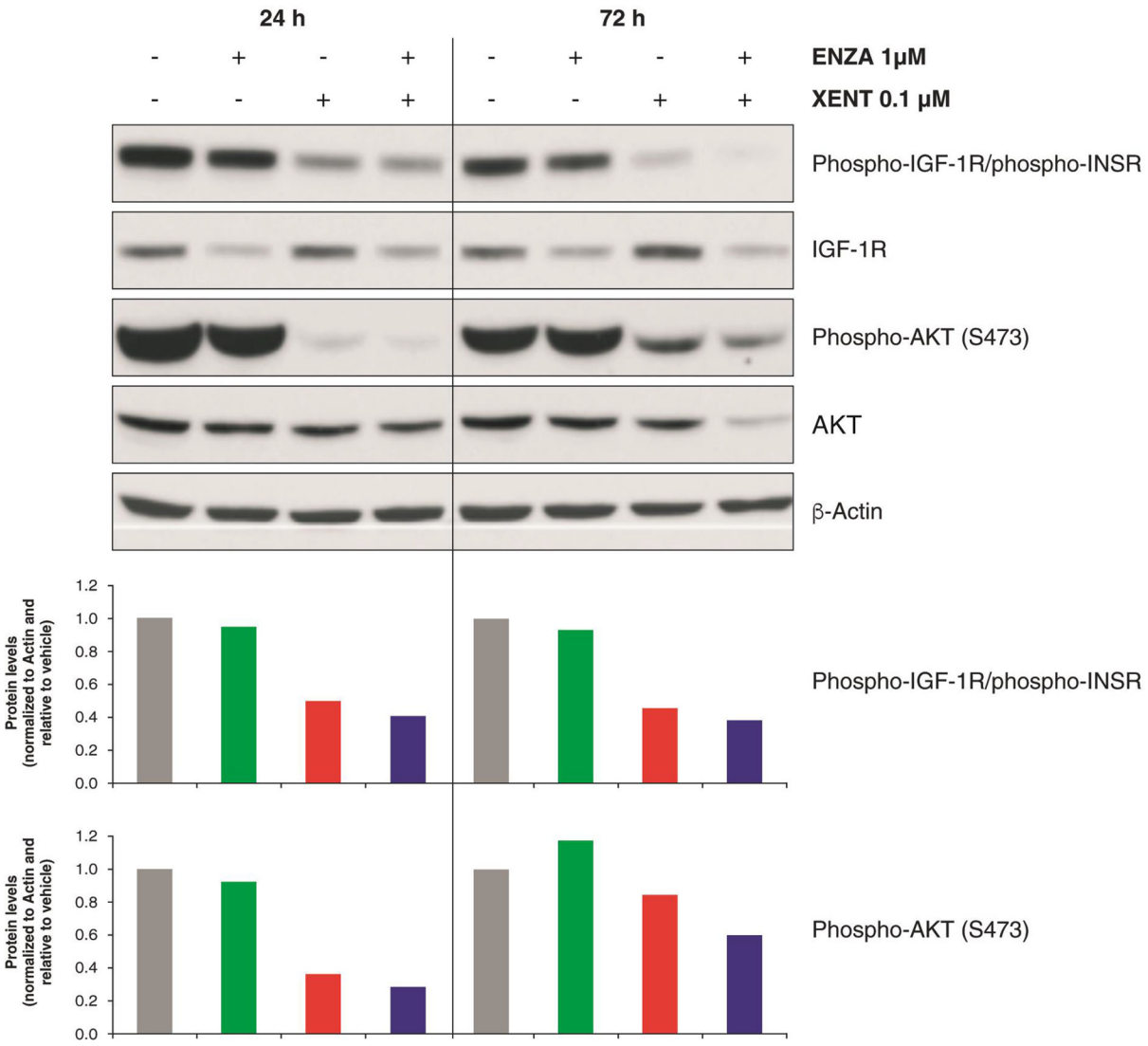

Figure 2.

IGF signaling: Effect of XENT and ENZA, alone or in combination, on IGF-1R and AKT phosphorylation status in VCaP cells. Cells were incubated with inhibitors in FBS-containing medium (in the absence of androgen or growth factor supplementation). Whole-cell lysates were prepared at indicated time points post-treatment and assessed by Western blot analysis. Quantitative analysis of protein bands was performed using the image analysis software ImageQuant TL 8.1.

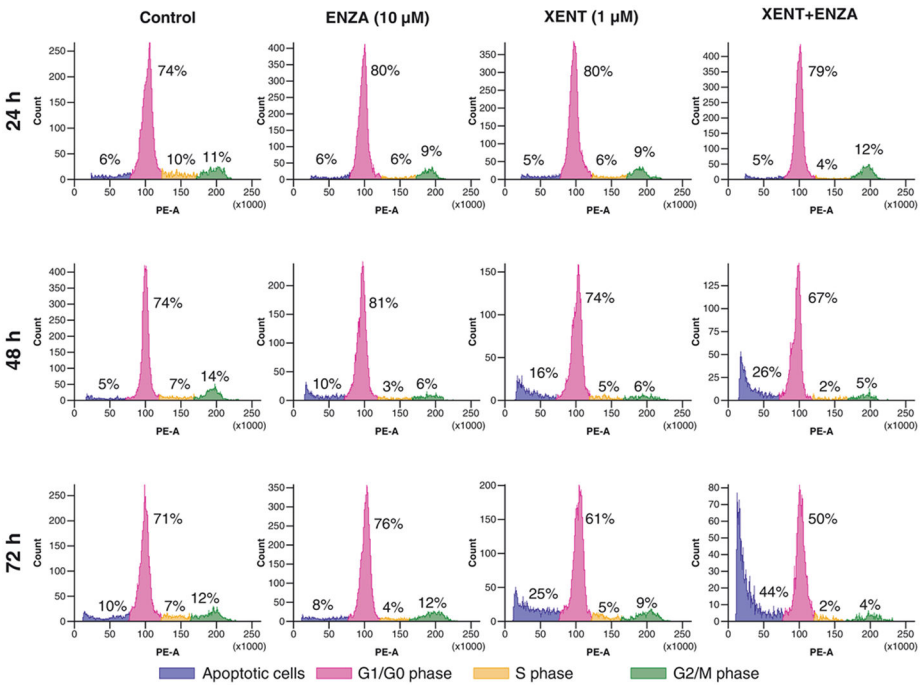

Figure 3.

Effect of XENT and ENZA, alone or in combination, on the cell-cycle profile of VCaP cells. Cells were incubated with inhibitors in FBS-containing medium (without androgen or growth factor supplementation) as indicated, fixed, stained (propidium iodide), and analyzed by flow cytometry.

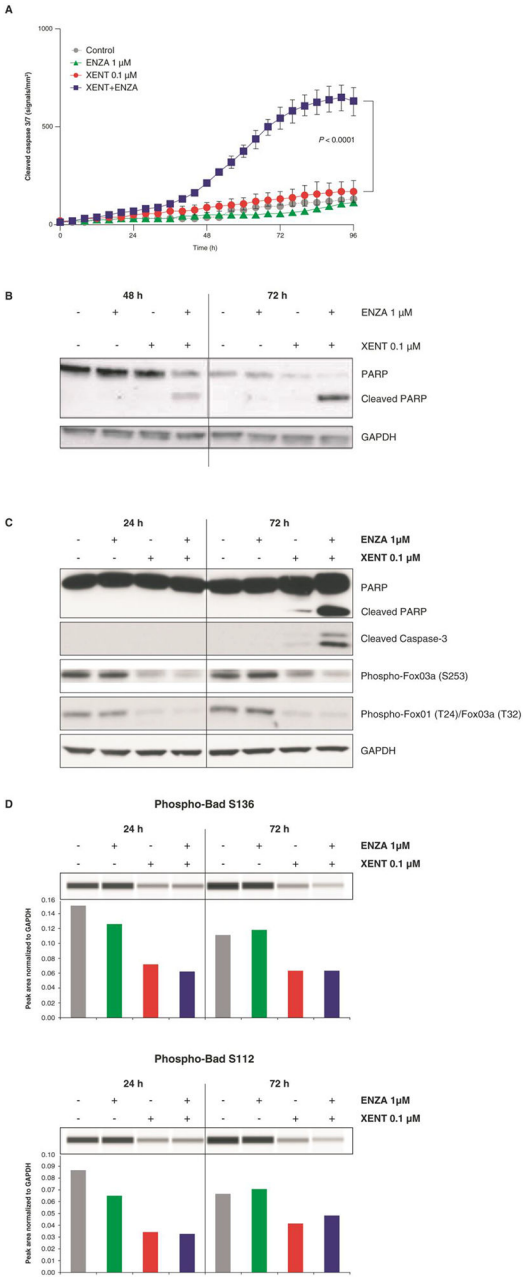

Figure 4.

Induction of apoptosis in VCaP cells: Effect of XENT and ENZA, alone or in combination, on caspase activity (A, C), cleaved PARP (B, C), phosphorylation status of FoxO3a/FoxO1 (C), and Bad (D). Cells were incubated with inhibitors as indicated in FBS-containing medium (without androgen or growth factor supplementation). Caspase-mediated apoptosis was detected using IncuCyte™ Caspase-3/7 Reagent and Western blot analysis. *P* values were calculated using pairwise t-tests (adjusted for multiplicity) following a one-way analysis of variance. Bad phosphorylation was determined by Simple Western™ quantification. All other proteins were assessed by Western blot analysis.

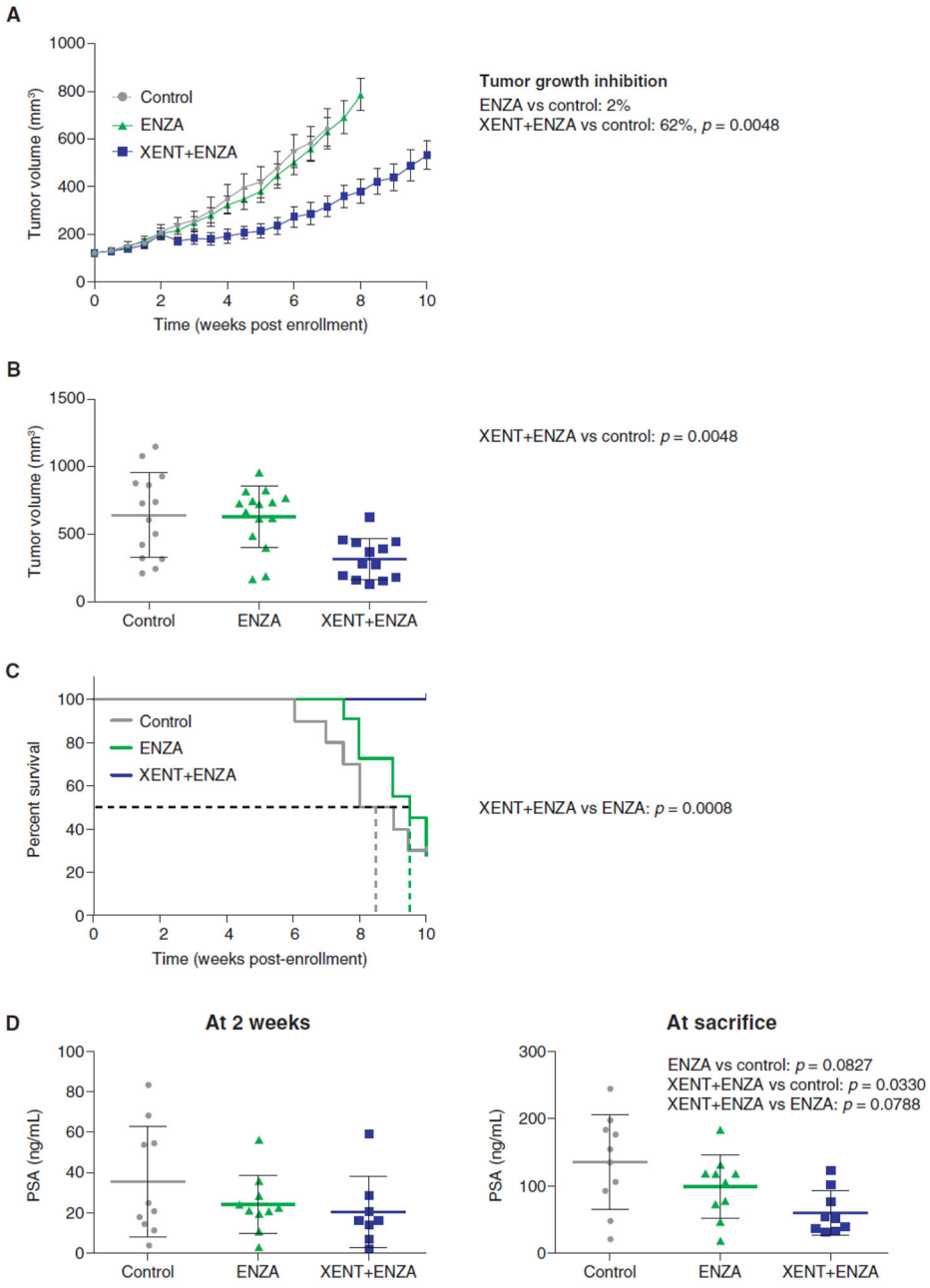

Figure 5.

In vivo tumor responses, survival, and PSA in LuCaP 96CR PDX. Fox Chase CB17 SCID male mice were castrated and were implanted with LuCaP 96CR tumor fragments 2 weeks later. Once tumor volumes exceeded 101 mm^3, animals were randomized to receive Natrosol™ vehicle control [p.o.; $n = 15$], ENZA (30 mg/kg p.o.; 5 days on, 2 days off, for 10 cycles; $n = 15$), or ENZA (dosing regimen as previously noted) plus XENT [200 mg/kg i.p., once weekly for 10 cycles; $n = 14$]. A) Change in tumor volume with time by treatment group; adjusted *P* values were calculated 7 weeks after start of treatment. B) Dot plot of tumor volumes in individual animals, by treatment group, 7 weeks after start of treatment. C) Survival by treatment group. D) Individual serum PSA levels, at 2 weeks of treatment,

and at sacrifice. *P* values were calculated using one-sided decreasing Mann–Whitney tests (adjusted according to Bonferroni–Holm).

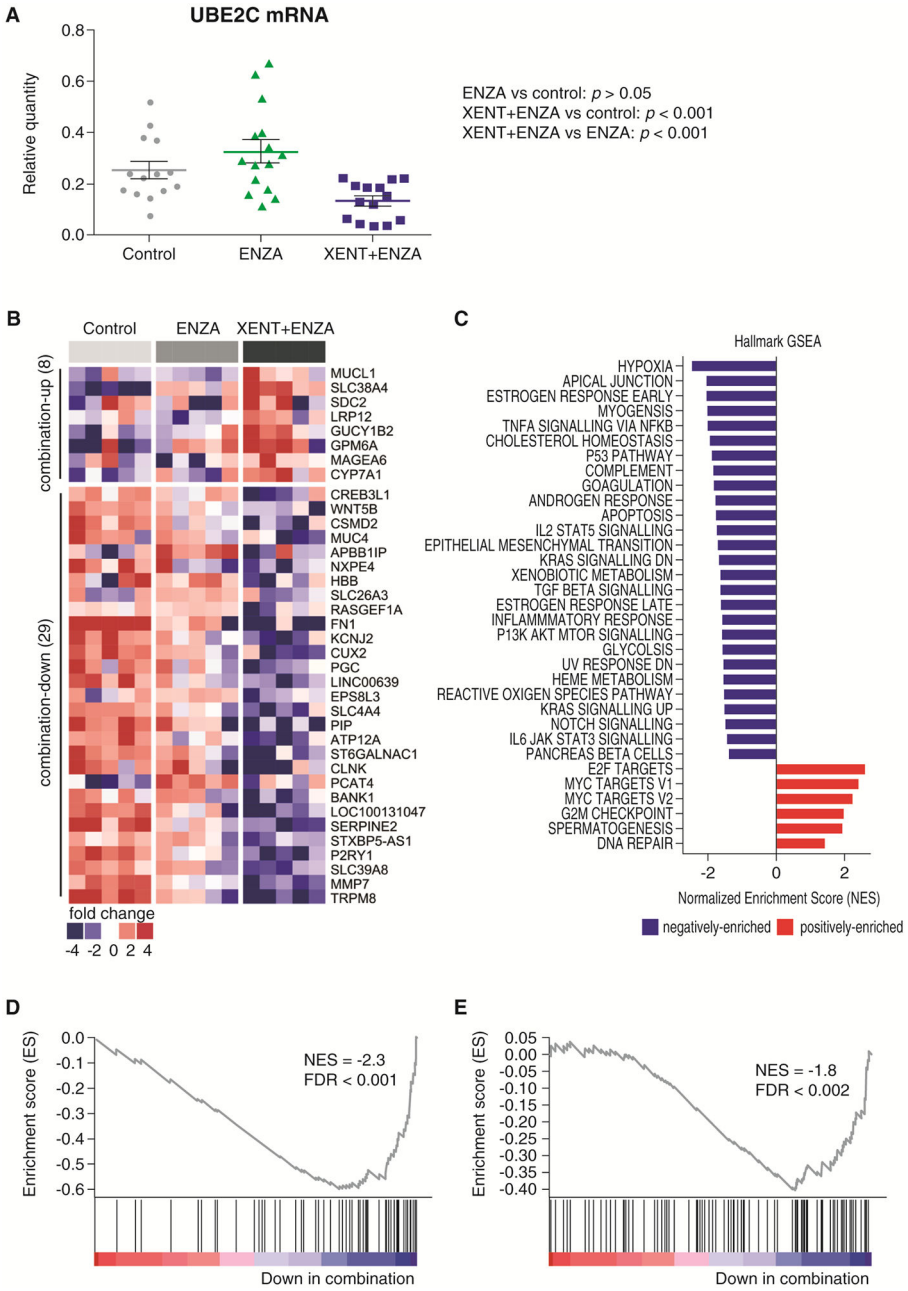

Figure 6.

Expression of the AR-V7 target gene UBE2C and RNA-Seq/GSEA in LuCaP 96CR PDX. A) qPCR analysis of UBE2C mRNA. B) Heat map of RNA-Seq data comparing vehicle control, ENZA, and the combination of XENT and ENZA for genes with $P < 0.05$ and fold change ≥ 3. C) GSEA results of all Hallmark pathways with FDR < 0.05. D) GSEA plot of HIF1 pathway. E) GSEA plot of androgen response genes. *P* values were calculated using Tukey tests conducted following a one-way analysis of variance.